Association Aéronautique et Astronautique de France

"Towards Sustainable Aviation" Summit
28 – 30 January 2025, Toulouse - France

Conceptual Aircraft Design and AI: Developing a functional relationship for the rapid realisation of future drone concepts

Mars Burke [(1)] and Alvin Gatto[(2)]
[(1)]Dept. of Mechanical and Aerospace Engineering, Brunel University London, Uxbridge, Middlesex, UB8 3PH, UK, Email:mars.burke@brunel.ac.uk, Email:alvin.gatto@brunel.ac.uk
[(2)]Dept. of Mechanical and Aerospace Engineering, Brunel University London, Uxbridge, Middlesex, UB8 3PH, UK, Email:alvin.gatto@brunel.ac.uk

ABSTRACT

The use of Unmanned Aerial Vehicles(UAVs) has expanded rapidly over the last decade. These systems have an almost limitless scope of application with resupply, surveillance, monitoring, and logistics representing but a few. Having such a wide scope, a means to rapidly, efficiently and accurately develop new designs fit-for-purpose would offer a significant advantage to developers given their inherent need to maximise potential within a competitive marketplace. This paper attempts to leverage the capabilities of Artificial Intelligence(AI) for this purpose through the development of functional synergies to predict maximum rated engine power from limited inputs and datasets. Overall, the use of AI techniques was found to offer the potential to substantial improve and enhance the design process with also the possibility for the creation of more cost-effective and efficient software tools that could significantly streamline the process.

1. INTRODUCTION

Artificial intelligence (AI) has become a transformative tool in aircraft design, addressing the growing complexity of systems and the need for optimization across multiple disciplines. From aerodynamics and propulsion to structural integrity and systems integration, AI techniques have proven instrumental in enabling faster, more efficient, and innovative designs.

The integration of AI into aerodynamic optimization is one area of particular note widely considered. Traditional aerodynamic design relies on computationally expensive methods like computational fluid dynamics (CFD) or wind tunnel testing, which often limit the scope of exploration in the design space. AI techniques have emerged as a practical alternative, reducing computational costs while maintaining accuracy. Techniques such as genetic algorithms (GAs) have emerged as powerful tools for navigating such complex design spaces, enabling a multi-objective optimization formulation by simultaneously considering dissimilar variables like aerodynamic performance, structural weight, and fuel efficiency. Haryanto et al. (2014) demonstrated the use of such techniques to optimize airfoil configurations for maximum lift-to-drag ratios, allowing for significant performance gains while reducing computational demand. Similarly, Duvigneau and Visonneau (2004) combined GAs with artificial neural networks (ANNs) to create hybrid optimization frameworks, leveraging the exploratory capabilities of GAs with the predictive efficiency of ANNs.

Wei et al. (2024) also used NNs when introducing DeepGeo, a neural network-based framework that simultaneously optimized shape and mesh deformation. This model was found to simplify the parameterization process, allowing for faster convergence to optimal aerodynamic designs. Their study also highlighted the potential of AI to directly handle high-dimensional geometric and aerodynamic variables, making it a valuable tool for complex design scenarios. Similarly, Mandia et al. (2024) demonstrated the use of multi-fidelity modelling in optimizing winglet configurations. By combining high and low-resolution datasets, their approach was considered to have achieved a balance between computational efficiency and predictive accuracy; both critical factors in early aircraft design stages. Another study by Ghoreyshi et al. (2024) further explored reduced-order modelling techniques such as Proper Orthogonal Decomposition (POD), undertaking efforts to simplify the often very complex flow dynamics into manageable computational problems, further accelerating the design process. Osco et al. (2021) has also demonstrated the use of Convolutional Neural networks(CNNs) to identify flow patterns and predict aerodynamic coefficients, significantly reducing the need for extensive simulations.

Predictive modelling is another domain where AI has made significant contributions, particularly in evaluating aircraft performance metrics. Predictive tools developed using AI can facilitate the rapid assessment of multiple design candidates, enabling more informed decision-making during conceptual and preliminary design phases. Trani et al. (2004) applied artificial neural networks to model fuel consumption across different

flight phases, achieving high predictive accuracy. These models could allow designers to evaluate the fuel efficiency of various configurations without relying on costly physical tests or simulations. Similarly, Tong (2020) employed machine learning algorithms to predict thrust-specific fuel consumption (TSFC) and engine core size, providing a reliable framework for optimizing propulsion systems.

The use of reinforcement learning in aircraft design has also shown considerable promise. Unlike traditional optimization methods, reinforcement learning adapts dynamically to feedback, allowing for iterative refinement of designs. Zhang et al. (2024) applied deep reinforcement learning to wing optimization, demonstrating its ability to evolve configurations that achieve superior aerodynamic efficiency compared to conventional approaches. By simulating complex flow environments, these algorithms refine design parameters to optimize performance metrics such as lift, drag, and stability characteristics. This adaptability makes reinforcement learning particularly valuable for addressing non-linear, multi-objective challenges inherent in aircraft design.

In addition to optimization, AI has been instrumental in addressing challenges related to structural design and materials. Similarly, the design of lightweight yet strong aircraft structures also involves balancing competing objectives such as load-bearing capacity, fatigue resistance, and manufacturability. Azizi Oroumieh et al. (2013) employed fuzzy logic and neural networks to model key structural parameters for light business jets. By leveraging AI, engineers can identify optimal configurations that balance competing objectives, streamlining the development process and reducing costs. Machine learning algorithms, including support vector machines and decision trees, have also been used to model and predict material properties based on experimental and computational data(Sun & Wang, 2019). Transfer learning, which leverages pre-trained models for new tasks, has been particularly effective in this area, enabling researchers to apply insights from existing datasets to new material systems (Dong & Ai, 2023).

The role of AI within the design space also extends to encompass integrated system design. Modern aircraft comprise highly interconnected subsystems, including propulsion units, avionics, and environmental controls. Coordinating these subsystems to achieve optimal performance necessitates sophisticated optimization frameworks. Garriga et al. (2019) developed an AI-enabled multi-disciplinary platform that evaluates aircraft configurations at varying fidelity levels. This system was deployed in advancing electrification of primary flight control systems and landing gear, aligning with the industry's push toward sustainable aviation. Multi-objective optimization frameworks that incorporate AI techniques have also been successfully applied to balance subsystem interactions (Haryanto et al., 2014) as well as reinforcement learning to manage trade-offs between conflicting design goals, such as maximizing thrust while minimizing noise pollution (Zhang et al., 2024).

Autonomous systems design has also emerged as a critical area of research within AI-driven aircraft design. UAVs are increasingly incorporating autonomous design features, requiring robust decision-making algorithms capable of handling dynamic environments. Within this theme, Reinforcement learning and fuzzy logic systems have been applied to optimize control strategies for autonomous flight (Ali, 1990). These methods enable adaptive behaviour, such as real-time trajectory adjustments and mission planning, enhancing the reliability and efficiency of autonomous systems. Explainable AI techniques, like SHAP and LIME, are also being integrated into these systems to provide transparency in decision-making processes, an important precursor to adequately addressing regulatory and safety concerns (Ramrao et al., 2023; Sun & Wang, 2019).

Data-driven approaches have further expanded the scope of AI in aircraft design. The vast amounts of data generated during design and testing phases, including telemetry, wind tunnel experiments, and CFD simulations, provide a rich foundation for machine learning models. Gradient boosting and ensemble methods have been employed to analyze these datasets, extracting actionable insights that inform design decisions (Dong & Ai, 2023). Transfer learning has enabled the application of insights from one domain to another, such as adapting UAV design principles to commercial aviation applications (Sun et al., 2019). Transformer architectures, with their ability to process sequential data, have also been explored for applications such as dynamic load prediction and flutter analysis (Li et al., 2023).

Despite its successes, the use of AI in aircraft design faces several challenges. One significant issue is the interpretability of AI models, particularly in safety-critical applications. Black-box models, while potentially accurate, often lack the transparency needed for regulatory approval and operational trust (Ali, 1990; Brunton et al., 2021). Some techniques seek to offer solutions to these issues by providing interpretable explanations for model predictions, however, their integration into complex design workflows continues to remain ongoing.

Data availability and quality are further challenges, particularly in early-stage design. High-fidelity data required for training machine learning models is often scarce and/or expensive to obtain. Synthetic data generation and data augmentation techniques are gaining some traction through solutions enabling researchers to simulate realistic datasets that enhance model robustness (Duvigneau & Visonneau, 2004; Mandia et al., 2024). Computational efficiency also remains a significant

concern, especially for real-time applications. While surrogate models and reduced-order methods have mitigated some of these challenges, scaling AI frameworks to handle the growing complexity of aircraft systems still requires further consideration(Haryanto et al., 2014; Kou & Zhang, 2023).

This work aims to explore and leverage the use of AI in developing a functional relationship for the prediction of maximum rated engine power for bespoke UAV platforms. To that end, this work describes; 1) the formulation, manipulation, characterisation, and rational behind the generation of the baseline dataset; 2) use of this dataset for the deployment and training of a developed AI architecture for future adoption within a more streamlined and efficient conceptual design process; 3) subsequent efforts at both verification and validation, and lastly; 4) overall assessments of the capabilities of the method for this purpose and identification of a suitable architecture construct.

2. DATABASE CHARACTERISATION

The database used for all subsequent analysis included a array of 96 individual UAV platforms of varying configuration, type, and application. Rotary wing configurations were not included with sole focus centred on traditional fixed-wing variants. One of the main aims of the database was to seek out and include as many relevant examples over as varied and diverse range as possible to ensure maximum applicability and representation to future developed models. The scope therefore was deliberately selected to encompass from the nano/micro sector(< 0.3 m) through to the large UAV category(~ 30 m) and see if Machine learning methodology use is appropriate and worthwhile. All information collated for the database was obtained from both online and reference text sources(Janes, 2024) with online information typically derived directly from the manufacturer.

After completion, the database included UAV platforms dating back to the late 1950's through to present day. Countries of origin were taken from examples all over the world with entry into service including operational status both active and retired. Also included were examples which are within active development and or production. In total UAVs that were/are manufactured from all over the world by many individual companies were cited with specified ranges(R) extending from 1.5 km to 3324 km, endurance(E) from 15min to 2400min, maximum rated engine powers(P) between 9W to 895kW, wing spans(S) from 0.15m to 26m and maximum operational altitudes(Alt) of between 0m to 16km above ground level Propulsion layouts included both tractor and pusher propellers operating both electric and internal combustion engine powerplant sources. Many were catapult launched variants (i.e electric, hydraulic, pneumatic), with other possessing a conventional landing functionality, parachute, airbag, parafoil recovery systems, deep-stall, automated belly landers, or skids as a landing mechanism. Both high tail configurations, low tail with a high wing and low wing inclusive are included. A select few had an offensive/attack capability/mission set with some armament deployment functionality, with others tasked within an Intelligence, Surveillance and/or Reconnaissance (ISR) remit.

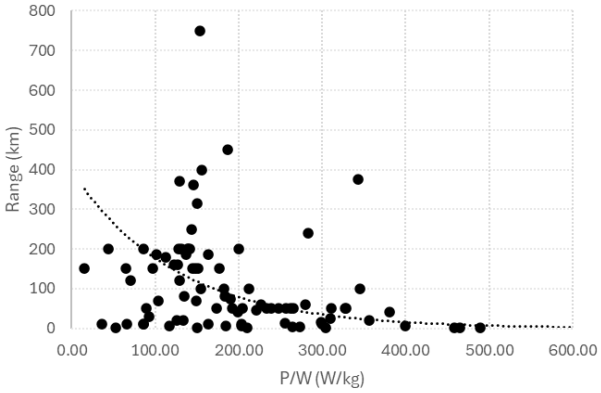

Figure 1. Range vs P/W ratio

3. BASIC TRENDS AND CORRELATIONS

Before deploying higher order models, cursory examination of the general trends existing within the dataset was considered worthwhile in order to establish any obvious characteristics and relationships. This analysis would also be beneficial, at the very least anecdotally, in establishing if the presented comparisons meet with general qualitative expectations. For this purpose, Figures 1-6 show various performance and baseline metric comparisons representative of those that could be specified early within an initial conceptual design phase as a result of customer drone requirements and needs. Included are range, endurance, maximum altitude and speed, all compared against maximum rated engine power normalised by MTOW[1] as well as wing span verses overall length. These metrics represented the most cited parameters from the various sources consulted during dataset assembly with other metrics much more difficult to obtain in the required quantities for widespread characterisation. On first inspection, significant data scatter within most figures is characteristic, making trend and correlation identification somewhat challenging. This is particularly evident within Fig. 1 highlighting Range and P/W. Overall, results tend to suggest for the varied array of platforms included, a wide bandwidth of Ranges exist across all P/W ratios presented with the possible exception of the highest P/W. In this case, appearance

[1] Not to be confused with the inverse of power loading defined as 'current' platform weight divided by generated horsepower.

seems to favour lower range expectations. This appears somewhat logical at first glance as higher P/W may suggest a higher energy consumption, and possibly, less efficient flight characteristics. Another feature of potential interest is the apparent wide scope of achievable ranges($0 < R < 800$km) for P/W $\approx$ 150 W/kg leading to the possible conclusion that this may represent an ideal operating point within this particular dataset. It should be remembered however, that datapoint number supporting this assertion remains relatively low and a more extensive dataset is needed for absolute confirmation. Overall, the indicative trend tends to suggest lower range capabilities with increasing P/W.

Figure 2 highlighting the relationship between endurance and P/W shows similar attributes. In this instance however, significantly greater indicative data scatter appears to exists at lower P/W (< 250 W/kg). Within this region, the scope of achievable endurance is large seemingly encompassing just minutes to many hours. Results also appear to suggest, in general agreement with Figure 1, that endurance is inversely correlated to P/W with distinctly lower endurance values at higher P/W ratios. Somewhat expectedly, these particular characteristics appear to confirm that focus on platform metrics and features towards flight efficiency and energy consumption are important considerations in determining overall flight endurance.

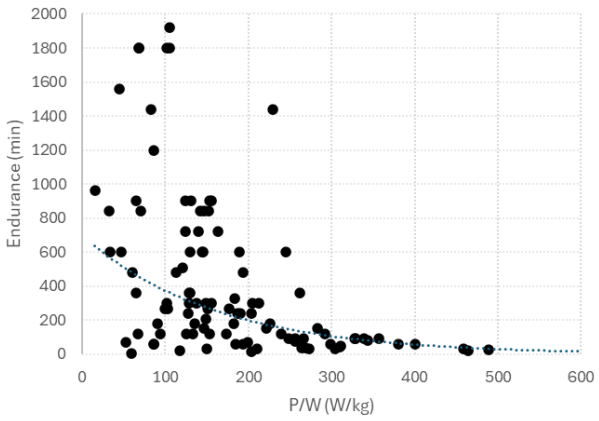

Figure 2. Endurance vs P/W ratio

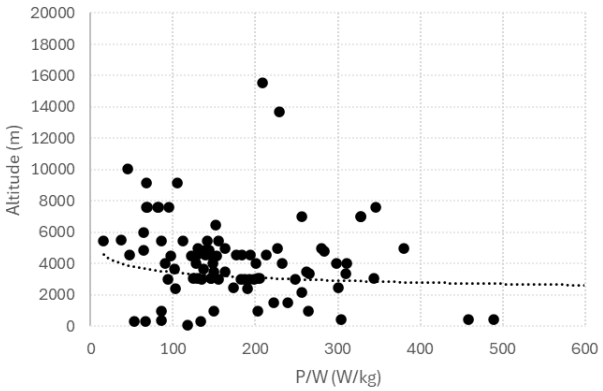

Figure 3. Altitude vs P/W ratio

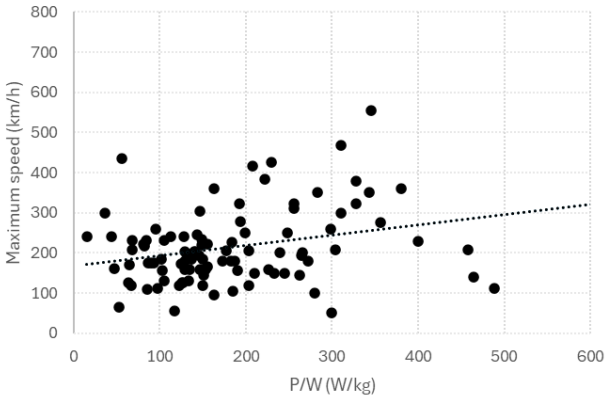

Figure 4. Maximum speed vs P/W ratio

The variation of Altitude with P/W continues the overarching trend of observed data scatter(Fig. 3). In this case, notwithstanding some data outliers, altitude also appears to be loosely correlated with the inverse of P/W ratio. This seems to further reinforce the obvious basic premise that flight efficiency and minimising energy consumption are important as well as the well know fact that engine power output normally decreases with increase in altitude.

A seemingly more obvious trend is evident in Figure 4 which shows the relationship between maximum level speed and P/W. In this case, and while significant data scatter remains, achievable maximum speed appears generally correlated with increasing P/W. This result would also tend to agree with expectations given higher P/W platforms would normally be designed, along with a higher wing loading, for such applications.

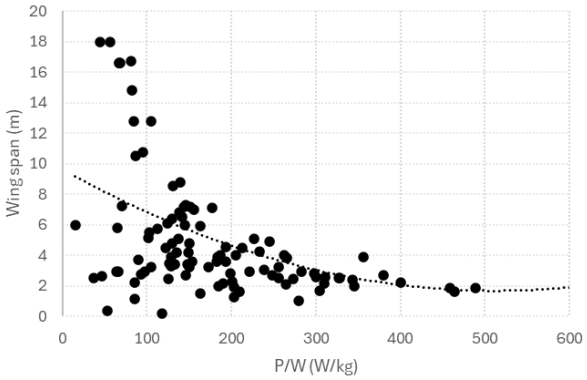

Figure 5. Wing span vs P/W ratio

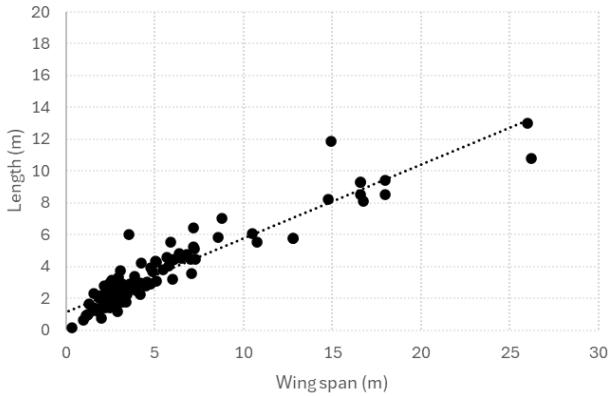

Figure 6. Overall length vs Wing span

Fig. 5 further supports this premise providing additional supporting evidence that smaller wing span configurations are correlated with higher P/W ratio. This relationship again appears much more variable and uncertain at lower values of P/W but at higher P/W, appear much less so. A more obvious correlation is also shown in Figure 6 with overall platform UAV length and wing span. This is remarkably well defined within the chosen dataset with platform length approximately half that of specified wing span.

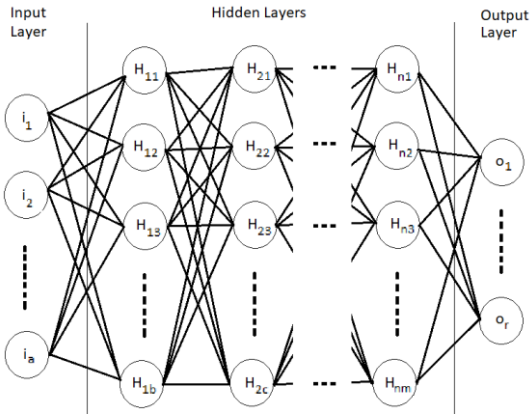

Figure 7. Generalised simple ANN structure

4. AI MODEL ARCHITECTURE

The machine learning model chosen for all subsequent analysis was a Feedforward Neural Network (FNN). This type of artificial neural network(ANN) attempts to effectively map the relationship between a set of input parameters to target outputs modelled on the working of the human brain (Khanna,1996). Figure 7 shows a generalised structure composed of an input layer(i) of depth a, n hidden layers, each with its own individual depth(in this case b, c, and for the nth layer, m), and a final output layer, o, of depth r. Each hidden neuron is characterised as a summation node with individual weights from each preceding neuron(along with a bias) fed forward through a non-linear activation function to subsequent layers. Error assessments are then made and weights modified thereafter for another subsequent cycle. This process is repeated continuously using the complete dataset(epoch) until acceptable or set fidelity is achieved. Typically, the dataset is presplit into training/validation/test sets (i.e 70/15/15 split); the former used to learn data characteristics; validation used to assess model performance on as yet unseen data points and to tune hyperparameters; with the latter, to test and assess the final trained and fine-tuned validated model against another independent set of data. This methodology was adopted here.

Various accuracy metrics can be used to assess network performance each with its own advantages and disadvantages. Ultimately, this choice depends largely on either the goals of the modelling and/or dataset character. In this instance, a combination of Mean Squared Error(MSE), Mean Averaged Percentage Error (MAPE) and R-sqaured metrics were used to assess overall model capabilities and fitness for purpose.

MSE remains one of the most common metrics for assessing predictive accuracy within regression applications with MSE representing the average squared difference between the predicted($\hat{y}_i$) and target(y_i) values over N samples(Eq.1). The aim of using this model is to minimize MSE with better indicative performance achieved with smaller MSE. MAPE is similar to MSE, however in this case the percentage error between the predicted($\hat{y}_i$) and target(y_i) values is calculated and averaged over N samples(Eq. 2). This model therefore gives a similar perspective to MSE but is notably a reference to dependent variable magnitude. As such, datasets with zero of infinite entries need to be avoided. Finally, R-squared uses a Sum of Squares of Errors (SSE) to the Total Sum of Squares (SST) relationship (Eq. 3) to indicate how closely two datasets relate to one another. Overall, R-squared has a maximum of one for perfectly fit data with below that (including less than zero) suggesting the model cannot fully represent the data characteristics.

$$MSE = \frac{1}{N}\sum_{i=1}^{N}(y_i - \hat{y}_i)^2 \quad \text{(Eq. 1)}$$

$$MAPE = \frac{1}{N}\sum_{i=1}^{N}\left(\left|\frac{y_i - \hat{y}_i}{y_i}\right| \text{ x } 100\right) \quad \text{(Eq. 2)}$$

$$R^2 = 1 - \frac{SSE}{SST} \quad \text{(Eq. 3)}$$

5. TRAINING, VALIDATION AND TESTING

To train and validate the selected AI model architecture, an iterative, automated process, was developed and applied to encompass a wide array of hidden layer and neurons number per layer. Various parameters including the influence of dropout and epoch number were also considered, albeit for the latter, most training and validation occurred at an imposed limit of 2000 epochs as a trade-off between computational resources and achievable model performance. Within this optimisation loop, the number of hidden layers was varied from one to ten with each layer containing up to a maximum of 50 neurons each. Given the scope of the investigation and to minimise training time scales, the number of neurons in each hidden layer was configured to be identical per layer as the indexing process took place each time. Five inputs(MTOW, S, R, E, and V) and one output(P) were nominally using to construct the model.

The training and validation methodology adopted deployed supervised learning on proportionally split, normalised, randomly shuffled, data segments in each case(70%/15%). A further data segment(15%) processed in a similar way was also split for test use; this set representing a further independent, never before been seen, number of example cases. Prior shuffling of the data ensured captured, unrelated patterns within data that were order-based were omitted. This can be an important consideration particularly when dealing with relatively small, wide-ranging datasets. In this case, shuffling randomly rearranged the data order prior to each epoch ensuring no data order visibility during each epoch exists helping to promote generalization. During training, the FNN sought to minimise prediction errors by iteratively adjusting weights and biases using the Adam optimisation algorithm guided by a MSE loss function. All hidden layers used the ReLU activation function in order to capture the inherent complex, non-linear relationships within the dataset with the single node output layer deploying a linear activation function to provide predicted values. Unless otherwise indicated, a 20% dropout, where 20% of randomly selected neurons during training were deactivated encouraging network generalisation while limiting/preventing overfitting, was also used with every hidden layer. Throughout this process, the Gradient Descent algorithm was adopted to minimize the loss function via iterative parameter model weight and bias updating.

The final performance evaluation of the FFN against the test data subset used both MAPE and R-squared metrics to assess fidelity. Considered in unison, these metrics were considered most appropriate to provide insights into the network's capabilities in terms of accuracy and generalization. These results, combined with a parallel investigation into the impact of other configurable input parameters already cited was considered sufficient for the assessment of the value of this FNN methodology and approach to the future application goal within aircraft conceptual design.

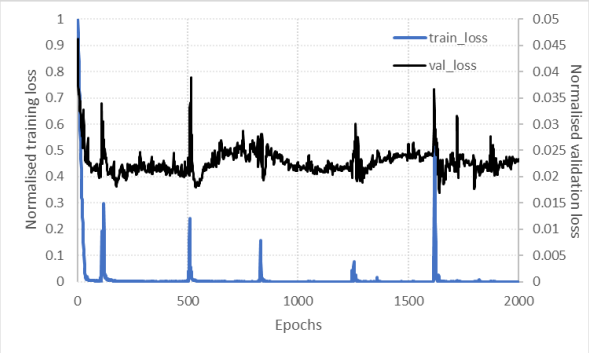

Figure 6. Training/validation loss results for 5-hidden-layer, 48 neuron FNN.

6. MODEL ASSESSMENT

The basic methodology adopted in developing the FNN was notionally one of exploratory investigation and interactive result interpretation with subsequent development/feedback. As a first step in this process, the initial model architecture was set to an upper limit of five hidden layers, with up to 50 neurons per layer, and 2000 epochs without dropout. Tab. 1 highlights the lowest final normalised MSE training and validation loss (including neuron numbers per hidden layer) as well as results indicating the best MAPE(lowest) and R-squared(highest) for the test data subset predictions. On first inspection, as would be expected, the level of training loss reduces with increase in hidden-layer count with the number of neurons per layer during this transition largely bias towards higher numbers approaching the maximum. Validation loss surprisingly seems much less sensitive to the same change seemingly reaching a minimum at 4 hidden layers with 27 neurons per layer. In each of these cases, it can be also be seen that although minimum MAPE results for the test subset are somewhat encouraging (and surprising at ≈1%), the related R-squared metric indicates very low correlated behaviour suggesting these particular model architectures are unlikely to represent and predict unseen test data adequately. Reasonable values of R-squared however do exist under these conditions when the number of neurons changes from 1 (albeit with very high relative training and validation losses), to 12, 24, and 46 then 42, suggesting, as would be expected, a higher

fidelity predictive trend with increase neuron count per hidden layer. To establish the character of the training/validation process, Fig. 6 shows this data with increasing epochs(minimum training loss case for 5 hidden layer and 48 neuron case – see Tab. 1).

Table 1. Results from initial up to 5 hidden layer, 50 neuron FNN(green highlights absolute minimum for this hidden layer configuration).

Hidden layers	Training loss	Validation loss	MAPE (%)	R-squared	No. Neurons
1	0.00013	0.0143	17.38	-5.499	49
	0.00051	0.0104	28.06	-1.724	15
	0.00016	0.0204	0.79	-2.941	40
	0.71846	0.3828	13.19	0.631	1
2	0.00010	0.0616	7.39	-5.641	22
	0.0008	0.0109	4.12	-2.389	47
	0.0018	0.0277	0.85	-2.210	46
	0.6045	0.0255	6.81	0.741	12
3	0.00009	0.0381	9.45	-0.272	39
	0.00015	0.0117	7.01	-3.221	32
	0.00017	0.0489	1.11	-3.988	22
	0.00073	0.0518	16.20	0.743	24
4	0.00007	0.0297	9.27	0.068	44
	0.00028	0.0073	8.46	0.416	27
	0.00051	0.0283	0.88	-6.846	9
	0.00168	0.0379	23.17	0.701	46
5	0.00005	0.0232	2.14	-0.264	48
	0.00154	0.0137	9.29	-8.87	18
	0.00204	0.1155	0.62	-3.16	7
	0.00043	0.0236	18.02	0.74	42

Table 2. Impact of data shuffle on the predictive capabilities of the FNN architecture.

Table 3. Impact of 20% dropout on the predictive capabilities of the FNN architecture.

Hidden layers	Training loss	Validation loss	MAPE (%)	R-squared	No. Neurons
1	0.00867	0.02687	13.92	0.421	36
	0.02921	0.01626	1.99	0.466	33
	0.02921	0.01626	1.99	0.466	33
	0.03436	0.03081	6.00	0.853	43
2	0.00795	0.02340	5.66	0.402	44
	0.06389	0.01751	11.96	0.438	41
	0.32273	0.02496	1.24	0.737	31
	0.91	0.04363	83.69	0.875	5
3	0.00779	0.02761	0.61	0.777	41
	0.02066	0.01297	79.00	-1.091	34
	0.00779	0.02761	0.61	0.777	41
	0.01512	0.01492	57.81	0.858	19
4	0.01094	0.02576	3.48	0.841	50
	0.23194	0.01276	42.05	0.777	17
	0.01902	0.02227	1.10	0.856	47
	0.07262	0.02340	16.82	0.907	47
5	0.01502	0.03149	20.30	0.89	40
	0.37961	0.01803	1.12	0.77	36
	0.01986	0.03707	0.79	0.77	47
	0.09459	0.02445	48.73	0.92	21

Dropout was the next influence considered. Tab. 3 shows these results with an applied 20% level. As can been seen, application of dropout seems to have a had a marked influence on R-squared with several instances of R-squared > 0.9. In each case, these model architectures seem to favour the higher hidden layer count and number of neurons(i.e R- squared = 0.907 and 0.92 for 4 and 5 hidden layers respectively). For the 4 hidden layer configuration, MAPE also shows encouraging predictive capabilities being 16.82%. Given these results, it appears that the application of dropout has materially improved model correlation beyond that of non-inclusion while maintaining adequate MAPE. It should also be noted that significantly lower MAPE is also observable with different architectures < 2% albeit with markedly lower, but still statistically reasonable R-squared(0.737-0.856 - utilising 31, 41, 47, and 47 neurons with 2, 3, 4, and 5 hidden layers respectively).

To further understand the achievable upper limit of R-squared, the maximum number of hidden layers was subsequently increased to 10 and the same model re-run. Tab. 4 highlights these results with both the training and validation losses relatively trendless however more importantly, R-squared shows relatively higher correlation magnitudes and consistency up until the addition of the 8th hidden layer before reducing with the 9th and 10th. The 8th hidden layer architecture (47 neurons) also indicated a reasonable MAPE at 11.26% with both training and validation losses near all-time lows for this setup. This seems to suggest that the best overall hidden layer number is 8 based on these metrics. To further highlight that this is indeed the case, Fig. 7 shows the extracted variation of R-squared against neuron number for this case. As indicated, R-squared appears to have plateaued and converged at just above 0.9 with no further improvement evident.

Table 4. Impact of additional hidden layers on the predictive capabilities of the FNN architecture.

Hidden layers	Training loss	Validation loss	MAPE (%)	R-squared	No. Neurons
6	0.01332	0.03413	48.59	0.896	50
	0.06352	0.02146	50.96	-8.361	38
	0.06539	0.02814	24.08	0.828	35
	0.03128	0.02483	43.63	0.912	42
7	0.01959	0.03991	122.77	0.768	44
	0.02168	0.02161	48.22	0.907	40
	0.17071	0.02361	7.20	0.834	49
	0.08083	0.02827	35.10	0.926	36
8	0.01933	0.03638	31.03	0.865	39
	0.10479	0.01543	78.18	0.868	46
	0.02703	0.01673	11.26	0.913	47
	0.02703	0.01673	11.26	0.913	47
9	0.01667	0.02992	98.64	0.691	50
	0.04286	0.01560	102.24	0.707	35
	0.15331	0.07574	65.81	-0.322	14
	0.08207	0.02819	85.33	0.870	39
10	0.02762	0.05626	73.37	0.49	42
	0.16797	0.02594	130.17	0.65	36
	0.06705	0.03779	48.33	0.80	49
	0.06705	0.03779	48.33	0.80	49

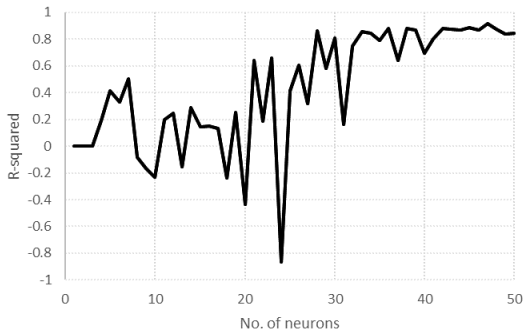

Figure 7. R-squared variation with number of neurons for the 8th hidden layer FFN.

As a final exploratory step, the number of epochs was increased from 2000 to 10000 for the same 8-hidden layer architecture to identify if any subsequent improvement was possible. Tab. 5 shows these results with the best R-squared showing consistency with Tab. 4 and Fig. 7 (at the same number of neurons), however it appears at the cost of a significantly increased MAPE. It seems therefore that no substantial extra correlation benefit is obtained with the extra computational cost of increasing epoch number for this model architecture.

Table 4. Results from 10000 epochs on the 8-hidden layer model architecture.

Hidden layers	Training loss	Validation loss	MAPE (%)	R-squared	No. Neurons
8	0.00856	0.02434	47.28	0.741	45
	0.01655	0.01710	39.21	0.746	35
	0.01172	0.02748	29.04	0.738	36
	0.02840	0.02168	57.69	0.91	47

7. CONCLUSIONS

Application of an AI machine learning feed-forward neural network to rapidly predict the maximum rated engine characteristics of UAV platforms has been presented. The architecture investigated for this problem involved using a single input layer consisting of five variables (maximum take-off weight, wing span, range, endurance, and maximum level speed) with a single output, maximum rated engine power. In between the input and output layers, a variable hidden layer architecture(up to 10) was constructed each containing up to a maximum of 50 neurons per layer. Other properties also assessed was the use of 20% dropout and epoch numbers up to 10000 from a baseline of 2000. Overall, the FNN architecture was found to predict the characteristics of the limited dataset used with reasonable fidelity. The optimal setup was identified as having 8 hidden layers with 20% dropout. Overall this configuration achieved a very reasonable 11.26% mean average percentage error and 0.913 R-square. Overall, this model performance gives some confidence that with further dataset expansion and model development, use of such techniques as a means for the rapid an efficient realisation of future drone platforms, within the initial conceptual design phase, is possible.

8. ACKNOWLEDGEMENTS

The work was financially supported under project "DATA3: Drone Design using AI for Transport Applications 3(Grant No 10126519)" as part of the UKRI Innovate UK Feasibility studies for AI solutions: Series 2 competition.

9. REFERENCES

1.Haryanto, I., Utomo, M. S. K. T. S., Sinaga, N., Rosalia, C. A., & Putra, A. P. (2014). Optimization of maximum lift to drag ratio on airfoil design based on artificial neural network utilizing genetic algorithm. Applied Mechanics and Materials, 493, 123-128. https://doi.org/10.4028/www.scientific.net/AMM.493.1

2.Duvigneau, R., & Visonneau, M. (2004). Hybrid Genetic Algorithms and Artificial Neural Networks for Complex Design Optimization in CFD. International Journal for Numerical Methods in Fluids, 44(11), 1257-1278. https://doi.org/10.1002/fld.741

3. Wei, Z., Yang, A., Li, J., Bauerheim, M., Liem, R. P., & Fua, P. (2024). DeepGeo: Deep Geometric Mapping for Automated and Effective Parameterization in Aerodynamic Shape Optimization. AIAA AVIATION FORUM AND ASCEND 2024. https://doi.org/10.2514/6.2024-3839

4. Mandia, V., Sharma, V., Chandra, Y., Kumar, G. and Singh, R.K. (2024), Optimizing Winglet Cant Angle for Enhanced Aircraft Wing Performance Using CFD Simulation and Hybrid ANN-GA. Int J Numer Meth Fluids. https://doi.org/10.1002/fld.5341

5. Ghoreyshi, M., Jirásek, A., & Cummings, R. M. (2013). Computational approximation of nonlinear unsteady aerodynamics using an aerodynamic model hierarchy. Aerospace Science and Technology, 28(1), 133–144. https://doi.org/10.1016/j.ast.2012.10.009

6. Osco, L. P., Marcato Junior, J., Marques Ramos, A. P., de Castro Jorge, L. A., Fatholahi, S. N., de Andrade Silva, J., Matsubara, E. T., Pistori, H., Gonçalves, W. N., & Li, J. (2021). A review on deep learning in UAV remote sensing. International Journal of Applied Earth Observation and Geoinformation, 102, 102456. https://doi.org/10.1016/j.jag.2021.102456

7. Trani, A., Wing-Ho, F., Schilling, G., Baik, H., & Seshadri, A. (2004). A neural network model to estimate aircraft fuel consumption. AIAA 4th Aviation Technology, Integration and Operations (ATIO) Forum,

Chicago, Illinois, 20–22 September 2004. https://doi.org/10.2514/6.2004-6401

8. Tong, M. T. (2020). Machine learning-based predictive analytics for aircraft engine conceptual design (NASA/TM-20205007448). National Aeronautics and Space Administration, Glenn Research Center.

9. Zhang, Z., Ao, Y., Li, S., & Gu, G. X. (2024). An adaptive machine learning-based optimization method in the aerodynamic analysis of a finite wing under various cruise conditions. Theoretical and Applied Mechanics Letters, 14, 100489,

10. Azizi Oroumieh, M. A., Malaek, S. M. B., Ashrafizaadeh, M., & Taheri, S. M. (2013). Aircraft design cycle time reduction using artificial intelligence. Aerospace Science and Technology, 26(1), 244-258. https://doi.org/10.1016/j.ast.2012.03.013

11. Sun, W., & Wang, L. (2019). A Review of Artificial Neural Network Surrogate Modeling in Aerodynamic Design. Aerospace Science and Technology, 93, Article 105332. https://doi.org/10.1016/j.ast.2019.105332

12. Garcia Garriga, A., Mainini, L., & Ponnusamy, S. S. (2019). A machine learning-enabled multi-fidelity platform for the integrated design of aircraft systems. Journal of Mechanical Design, 141(12), 121405. https://doi.org/10.1115/1.4044401

13. Ali, M. (1990). Intelligent systems in aerospace. The Knowledge Engineering Review, 5(3), 147-166. https://doi.org/10.1017/S0269888900005385

14. Ramrao, A., Subhash, T., & Pandurang, S. (2023). AI-Driven Predictive Maintenance for Aerospace Engines. Journal of Propulsion Technology, 19(2), 150-168. https://doi.org/10.1016/j.jproptech.2023.005202.

15. Dong, Y., & Ai, J. (2012). Research on estimating method of fuel and emissions using neural networks in LTO cycle for preliminary aircraft design. 28th International Congress of the Aeronautical Sciences (ICAS), Shanghai, China.

16. Brunton, S. L., Kutz, J. N., Manohar, K., Aravkin, A. Y., Morgansen, K., Klemisch, J., Goebel, N., Buttrick, J., Poskin, J., Blom-Schieber, A., Hogan, T. A., & McDonald, D. (2021). Data-driven aerospace engineering: Reframing the industry with machine learning. AIAA Journal, 59(7), 2820-2847. https://doi.org/10.2514/1.J060131

17. Kou, J., & Zhang, W. (2021). Data-driven modeling for unsteady aerodynamics and aeroelasticity. Progress in Aerospace Sciences, 125, 100725.

18. Khanna, T., “Foundations of Neural Networks.”, New York., Addison-Wesley., 1996.

19. Jane's All the World’s Aircraft: Unmanned Yearbook, 2024/2025 Edition, Jane's Group, ISBN9780710634474